AD-A237 024

Defense Nuclear Agency
Alexandria, VA 22310-3398

DNA-TR-90-71

Target Area Operating Conditions
Dust Lofting from Natural Surfaces

R. A. Gaj
R. D. Small
Pacific-Sierra Research Corporation
12340 Santa Monica Boulevard
Los Angeles, CA 90025-2587

DTIC
ELECTE
JUN 19 1991
S B D

June 1991

Technical Report

CONTRACT No. DNA 001-87-C-0298

Approved for public release;
distribution is unlimited.

91-02232

Destroy this report when it is no longer needed. Do not return to sender.

PLEASE NOTIFY THE DEFENSE NUCLEAR AGENCY, ATTN: CSTI, 6801 TELEGRAPH ROAD, ALEXANDRIA, VA 22310-3398, IF YOUR ADDRESS IS INCORRECT, IF YOU WISH IT DELETED FROM THE DISTRIBUTION LIST, OR IF THE ADDRESSEE IS NO LONGER EMPLOYED BY YOUR ORGANIZATION.

DNA PRINTING PLANT

DISTRIBUTION LIST UPDATE

This mailer is provided to enable DNA to maintain current distribution lists for reports. We would appreciate your providing the requested information.

☐ Add the individual listed to your distribution list.

☐ Delete the cited organization/individual.

☐ Change of address.

NOTE:
Please return the mailing label from the document so that any additions, changes, corrections or deletions can be made more easily.

NAME: _____

ORGANIZATION: _____

OLD ADDRESS	CURRENT ADDRESS
_____	_____
_____	_____
_____	_____

TELEPHONE NUMBER: ( ) _____

SUBJECT AREA(s) OF INTEREST:

_____ _____

_____ _____

_____ _____

DNA OR OTHER GOVERNMENT CONTRACT NUMBER: _____

CERTIFICATION OF NEED-TO-KNOW BY GOVERNMENT SPONSOR (if other than DNA):

SPONSORING ORGANIZATION: _____

CONTRACTING OFFICER OR REPRESENTATIVE: _____

SIGNATURE _____

CUT HERE AND RETURN

Director
Defense Nuclear Agency
ATTN: TITL
Washington, DC 20305-1000

Director
Defense Nuclear Agency
ATTN: TITL
Washington, DC 20305-1000

REPORT DOCUMENTATION PAGE

Form Approved
OMB No. 0704-0188

Public reporting burden for this collection of information is estimated to average 1 hour per response including the time for reviewing instructions, searching existing data sources, gathering and maintaining the data needed, and completing and reviewing the collection of information. Send comments regarding this burden estimate or any other aspect of this collection of information, including suggestions for reducing this burden, to Washington Headquarters Services Directorate for Information Operations and Reports, 1215 Jefferson Davis Highway Suite 1204, Arlington, VA 22202-4302, and to the Office of Management and Budget, Paperwork Reduction Project (0704-0188), Washington, DC 20503

1 AGENCY USE ONLY (Leave blank)	2 REPORT DATE	3. REPORT TYPE AND DATES COVERED
	910601	Technical 870929 - 900429

4. TITLE AND SUBTITLE

Target Area Operating Conditions
Dust Lofting from Natural Surfaces

5. FUNDING NUMBERS

C - DNA 001-87-C-0298
PE - 62715H
PR - RA
TA - RG
WU - DH044920

6. AUTHOR(S)

R. A. Gaj, R. D. Small

7 PERFORMING ORGANIZATION NAME(S) AND ADDRESS(ES)

Pacific-Sierra Research Corporation
12340 Santa Monica Boulevard
Los Angeles, CA 90025-2587

8 PERFORMING ORGANIZATION REPORT NUMBER

PSR Report 1817

9. SPONSORING/MONITORING AGENCY NAME(S) AND ADDRESS(ES)

Defense Nuclear Agency
6801 Telegraph Road
Alexandria, VA 22310-3398
SPWE/Gallaway

10. SPONSORING/MONITORING AGENCY REPORT NUMBER

DNA-TR-90-71

11. SUPPLEMENTARY NOTES

This work was sponsored by the Defense Nuclear Agency under RDT&E RMC Codes B4662D RA RG 00122 SPAS 3420A 25904D and B4662D RA RG 10122 SPWE 4400A 25904D.

12a DISTRIBUTION/AVAILABILITY STATEMENT

Approved for public release; distribution is unlimited.

12b. DISTRIBUTION CODE

13 ABSTRACT *(Maximum 200 words)*

We explore how variations in soil type, vegetation cover, and climatic conditions influence the sweepup mass in target regions. A simple dust sweepup/suspension model, appropriate for the high wind speeds associated with nuclear blast waves, is developed to depend explicitly on the threshold shear velocity required to initiate dust lofting. Given an analytic driver for the positive phase free stream wind speed versus ground range and time, sweepup masses for a wide range of surface types and conditions are calculated. We find that for an airburst at SHOB = 500 ft/KT$^{1/3}$, the sweepup mass can be reduced to near zero if the surface is covered with tall grass or a mature small grain crop. For bursts over loose, unvegetated sand, sweepup efficiencies are nearly six times greater than for a typical Nevada Test Site surface. For a lower altitude airburst (SHOB = 50 ft/KT$^{1/3}$), a somewhat smaller variation between these extremes is predicted (e.g., scouring is possible even over grass or cropland). The yield dependence of sweepup mass and the surface area scoured by the blast winds is also explored. The results indicate that the net dust injection from a nuclear laydown can vary significantly within individual target areas and may be a strong function of season—especially in agricultural regions.

14 SUBJECT TERMS

Sweepup	Soil	Target Areas
Scouring	Threshold Velocity	Vegetation
Dust Lofting	Boundary Layers	

15. NUMBER OF PAGES
38

16. PRICE CODE

17 SECURITY CLASSIFICATION OF REPORT	18 SECURITY CLASSIFICATION OF THIS PAGE	19. SECURITY CLASSIFICATION OF ABSTRACT	20. LIMITATION OF ABSTRACT
UNCLASSIFIED	UNCLASSIFIED	UNCLASSIFIED	SAR

NSN 7540-280-5500

Standard Form 298 (Rev 2-89)
Prescribed by ANSI Sta 239-18
298 102

CLASSIFIED BY:

N/A since Unclassified

DECLASSIFY ON;

N/A since Unclassified

PREFACE

Fratricide probabilities are derived from model predictions of nuclear clouds. Experimental data are sparse and alternative validations are needed. Pacific-Sierra Research Corporation (PSR) has examined several key issues where uncertainties are large and recommended validations for three such areas. They include: the influence of surface conditions on the sweepup mass of nuclear clouds; fireball quenching by entrained mass; and long range cloud transport.

In Vol. 1 of this report series, smoke plumes and obscurations above target areas were considered. Volume 2 considered long range dust transport and Saharan dust events as an analog for dispersion of nuclear clouds. Volume 3 recommends high energy experiments to simulate fireball-particle interactions.

In this volume, we develop an analysis for the mass entrained by nuclear clouds. Real soil moisture and vegetation cover are accounted for and it is demonstrated that sweepup mass in some target areas is considerably less than currently estimated.

This research was performed under contract DNA 001-87-C-0298 and monitored by Dr. Charles R. Gallaway, Shock Physics Weapon Effects, Defense Nuclear Agency.

DTIC COPY INSPECTED 5

Accession For
NTIS GRA&I ☑
DTIC TAB ☐
Unannounced ☐
Justification
By
Distribution/
Availability Codes
Dist | Avail and/or Special
A-1

CONVERSION TABLE

Conversion factors for U.S. customary to metric (SI) units of measurement

To Convert From	To	Multiply
angstrom	meters (m)	1.000 000 X E-10
atmosphere (normal)	kilo pascal (kPa)	1.013 25 X E+2
bar	kilo pascal (kPa)	1.000 000 X E+2
barn	meter^2 (m^2)	1.000 000 X E-28
British Thermal unit (thermochemical)	joule (J)	1.054 350 X E+3
calorie (thermochemical)	joule (J)	4.184 000
cal (thermochemical)/cm^2	mega joule/m^2(MJ/m^2)	4.184 000 X E-2
curie	giga becquerel (GBq)*	3.700 000 X E+1
degree (angle)	radian (rad)	1.745 329 X E-2
degree Fahrenheit	degree kelvin (K)	$t_K=(t°f + 459.67)/1.8$
electron volt	joule (J)	1.602 19 X E-19
erg	joule (J)	1.000 000 X E-7
erg/second	watt (W)	1.000 000 X E-7
foot	meter (m)	3.048 000 X E-1
foot-pound-force	joule (J)	1.355 818
gallon (U.S. liquid)	meter^3 (m^3)	3.785 412 X E-3
inch	meter (m)	2.540 000 X E-2
jerk	joule (J)	1.000 000 X E+9
joule/kilogram (J/Kg) (radiation dose absorbed)	Gray (Gy)	1.000 000
kilotons	terajoules	4.183
kip (1000 lbf)	newton (N)	4 448 222 X E+3
kip/inch^2 (ksi)	kilo pascal (kPa)	6.894 757 X E+3
ktap	newton-second/m^2 (N-s/m^2)	1.000 000 X E+2
micron	meter (m)	1.000 000 X E-6
mil	meter (m)	2.540 000 X E-5
mile (international)	meter (m)	1.609 344 X E+3
ounce	kilogram (kg)	2.834 952 X E-2
pound-force (lbf avoirdupois)	newton (N)	4.448 222
pound-force inch	newton-meter (N·m)	1.129 848 X E-1
pound-force/inch	newton/meter (N/m)	1.751 268 X E+2
pound-force/foot^2	kilo pascal (kPa)	4.788 026 X E-2
pound-force/inch^2 (psi)	kilo pascal (kPa)	6.894 757
pound-mass (lbm avoirdupois)	kilogram (kg)	4.535 924 X E-1
pound-mass-foot^2 (moment of inertia)	kilogram-meter^2 (kg m^2)	4.214 011 X E-2
pound-mass/foot^3	kilogram/meter^3 (kg/m^3)	1.601 846 X E+1
rad (radiation dose absorbed)	Gray (Gy)**	1.000 000 X E-2
roentgen	coulomb/kilogram (C/kg)	2.579 760 X E-4
shake	second (s)	1.000 000 X E-8
slug	kilogram (kg)	1.459 390 X E+1
torr (mm Hg, 0°C)	kilo pascal (kPa)	1.333 22 X E-1

*The becquerel (Bq) is the SI unit of radioactivity; Bp = 1 event/s.

**The Gray (Gy) is the SI unit of absorbed radiation.

TABLE OF CONTENTS

Section		Page
	PREFACE	iii
	CONVERSION TABLE	iv
	FIGURES	vi
1	INTRODUCTION	1
2	CLASSIFICATION OF SURFACE TYPES	2
	2.1 THRESHOLD SHEAR VELOCITY	2
	2.2 OBSERVED VARIATIONS	3
	2.3 SEASONAL VARIATIONS	4
	2.4 NUCLEAR INFLUENCES	6
3	SWEEPUP MODEL	8
	3.1 BACKGROUND	8
	3.2 HIGH SPEED MASS FLUX MODEL	8
4	SWEEPUP CALCULATIONS	11
	4.1 METHODOLOGY	11
	4.2 VARIATIONS IN SWEEPUP MASS	11
	4.3 VARIATIONS IN SWEEPUP RADIUS	13
	4.4 NEVADA TEST SITE SOIL	17
	4.5 NORMALIZED SWEEPUP MASS	21
5	IMPLICATIONS FOR TARGET AREAS	23
6	CONCLUSIONS	25
7	LIST OF REFERENCES	26

FIGURES

Figure		Page
1	Threshold shear velocity as function of season for U.S. agricultural area—loam soil	5
2	Threshold shear velocity as function of season for U.S. agricultural area—sandy soil	7
3	Blowing parameter as function of normalized shear stress	10
4	Net sweepup mass as function of threshold shear velocity	12
5	Net sweepup mass as function of burst altitude	14
6	Net sweepup mass as function of yield	15
7	Effective sweepup radius as function of threshold shear velocity	16
8	Effective sweepup radius as function of burst altitude	18
9	Effective sweepup radius as function of yield	19
10	Sweepup mass relative to airburst over Yucca Valley as function of threshold shear velocity	22
11	Soils in the Minot AFB, North Dakota ICBM silo area	24

SECTION 1

INTRODUCTION

The amount of dust and debris which can be scoured and lofted into a nuclear cloud depends strongly upon surface conditions in the target area. Regional and seasonal variations in land use, vegetative cover, soil moisture, and soil texture all influence the sweepup mass source and lead to wide differences in the mass injection. The dependencies are poorly understood and are not at present accounted for in any DNA sweepup model. As a result, broad uncertainties are introduced any time sweepup models are applied to target areas outside the region for which they were originally developed (namely, dry, sandy deserts). This is a serious problem, especially considering the geographic variety of strategic targets areas found in the Soviet Union (e.g., subarctic taiga forests, black soil farmland, wooded river valleys, and semiarid steppes). Sweepup from those regions can hardly be expected to resemble sweepup from a desert; but currently, it is impossible to distinguish the differences.

In this report, we calculate sweepup masses (without accounting for material fallback to the surface) for a wide range of surface conditions. Our approach has two main components: (1) A surface classification scheme based on measured *threshold shear velocities*, and (2) a theoretical mass flux model appropriate for the high surface wind speeds associated with nuclear blast waves. These two components are combined such that the vertical dust flux has an explicit dependence upon the threshold shear velocity. Time- and range-dependent nuclear blast winds are prescribed using analytic positive phase dynamic pressure formulae. Although our model is highly idealized (it cannot, for example, account for precursor flows or uneven terrain), the results nevertheless demonstrate the seriousness of ignoring regional and seasonal variations in target area conditions. Moreover, they indicate a clear direction for more detailed theoretical and experimental work.

The report is divided into six sections. In Sec. 2, we describe the surface classification scheme and discuss how threshold velocities can vary with soil type and season. Next, in Sec. 3, we describe the sweepup model. This model is then applied in Sec. 4 to calculate the total sweepup mass and the "effective scouring radius" for various surfaces, heights of burst, and yields. The implications of these results are discussed in Sec. 5, and conclusions presented in Sec. 6.

SECTION 2

CLASSIFICATION OF SURFACE TYPES

The blast winds generated by low altitude nuclear detonations are strong enough to scour material from virtually any natural surface. Dirt, pebbles, bushes—even rocks and trees—can be carried away when subjected to winds in excess of several hundred meters per second. Yet, while it is clear *some* sweep up will probably always occur (especially at ground ranges where dynamic pressures maximize), it is equally clear that the *amount* of material swept up is not the same for all surfaces. Vegetated land, for example, yields less sweepup mass than barren ground; and moist (or frozen) soil less than dry. The key issue is the ability of a surface to resist the shear stresses exerted by a nuclear blast wave and its accompanying winds. Any factor which either (a) lessens the stress applied directly to the soil (such as a plant cover), or (b) increases the cohesiveness of particulates lying on the surface (such as a high moisture content) tends to lessen the susceptibility of the soil to sweepup and thus reduce the net mass lofted. An explicit quantification of all those factors has not been developed; however, the threshold shear velocity can at least roughly categorize their net effect for a given surface.

2.1 THRESHOLD SHEAR VELOCITY.

The threshold shear velocity is a measure of the minimum shear stress required to initiate particle motion along the ground. It is experimentally determined in the field using a portable, open-bottomed wind tunnel with a regulated airflow [e.g., Gillette, 1978]. As the wind speed in the tunnel is increased from zero, the shear velocity

$$U_* \equiv \left(\tau_*/\rho\right)^{1/2} = k\frac{dU}{d\ln Z} \qquad (1)$$

is monitored until *saltation* (indicated by particles rolling or bouncing along the surface) begins.[1] Here τ_* is the shear stress, ρ is the air density, $k \approx 0.4$ is the von Karmann coefficient, and U is the horizontal wind speed at some height Z above the ground. The value of U_* at which saltation first occurs defines the threshold shear velocity U_{*th}.

The threshold shear velocity U_{*th} can also be used to define the point at which dust enters into *suspension*. This regime, defined by the condition [Owen, 1964]

$$\frac{U_*}{U_{*th}} \gtrsim 10 \ , \qquad (2)$$

begins when the turbulent drag force upon individual particles first exceeds their gravitational fall speed. It is at this point that the particles become lofted and can be carried to high altitude. Suspension is the mechanism which creates sand and dust storms in arid regions. It is also responsible for the dense sweepup layers generated by nuclear airbursts. Equation (2) therefore forms a base for the sweepup model described in Sec. 3.

1. The relation between shear stress and vertical wind shear given by Eq. (1) is strictly valid only when the atmospheric surface layer is statically neutral (well mixed). Corrections to this formula for other stability profiles are available [see Businger, 1973].

2.2 OBSERVED VARIATIONS.

The concept of using U_{*th} as an index for sweepup potential was originally developed for application to "normal" (non-nuclear) conditions such as dust erosion from drought-stricken agricultural land and deserts. Thus the only systematic measurements made to date have been over dry, barren, or sparsely vegetated ground, since such surfaces are most likely to be subject to significant low-wind speed sweepup. Nevertheless, even for this restricted range of surface types, wide variations in U_{*th} have been found.

Table 1 summarizes some of these variations. In general, soils which are loose (e.g., plowed or otherwise disturbed) or sandy are the most easily eroded (and thus have the lowest U_{*th}); loamy soils, soils with a large number of large elements such as pebbles and those with a crusted or cloddy surface are the least erodible. In most cases, mineral content also influences soil erosion potential. High concentrations of exchangeable sodium or calcium carbonate ($CaCO_3$), for example, tend to increase U_{*th} in clay soils by strengthening their crustal strength [Gillette, 1982].

All of the soils listed in Table 1 were dry. Technically, this means that the water content in the first few inches below the surface was at or below the *wilting point* for most crops. (The wilting point corresponds to a water to soil volume ratio of 0.05 for sandy loams, 0.08 for loam, and 0.17 for clay [Alderfer, 1977].) It has been found, however, that once the water content of a soil begins to exceed the wilting point (due to rainfall or irrigation), U_{*th} increases substantially above the values listed in Table 1, although it is not clear how much [Chepil, 1956]. Saturated or frozen soils are likely to be even more stable, but, again, no measurements are available.

Precipitation can modify the threshold velocity in other, although less obvious, ways. Sandy soils which are initially dry and cloddy, for example, often become *more* erodable several days to weeks after a heavy rainfall. This is due to the

Table 1. Mean threshold velocities for unvegetated soils.

	Threshold Shear Velocity (m/s)			Percent Mass in Particles >1 mm diameter		Modulus of Crustal Rupture (bars)
Soil Type	Loose	Cloddy	Crusted	Loose	Cloddy	
Sand	0.28	0.75	0.66	3	60	0.03
Sandy loam	0.29	1.05	2.90	30	64	0.42
Loamy sand	0.34	0.85	1.03	26	47	0.5
Clay	0.54	>1.50	>2.00	42	94	0.75
Silty Clay	0.56	----	----	6	--	----
Silty clay loam	0.64	----	>1.50	18	--	----
Clay loam	0.68	>1.09	1.20	28	81	0.38
Loam	0.78	>1.50	>1.50	49	89	0.66
Silt loam	1.08	>2.00	>1.50	77	89	0.8

Source: Gillette [1988].

tendency for rainfall to "melt" (disaggregate) the clods lying on the surface. Once the soil dries, it returns to a smooth, loose, and thus more easily eroded state. On the other hand, if the soil is initially loose, wetting and drying may ultimately lead to the formation of a crust, thereby *increasing* U_{*th}. Timing is an important issue here: If the surface is subjected to strong winds very soon after a rainfall (or snowmelt), significant drying of the upper few millimeters may occur before the crust can form. Sweepup can then follow, even though the soil a centimeter or two below the surface is still water-soaked. This effect has been observed many times in loam and clay loam soils [Gillette, 1988]. In a nuclear environment, thermal irradiation of the surface may also dry the upper soil horizon, possibly negating the stabilizing influence of soil moisture. (This influence could however be mitigated by a smoke, dust, or steam layer just above the surface which would tend to shield the ground.)

Very few measurements have been made of the effects of live vegetation upon sweepup. It has been found, however, that any sort of grass or small grain crop cover (e.g., wheat, barley, rye) is usually sufficient to preclude sweepup for all but the strongest natural winds $\left(U_* \gtrsim 2 \text{ m/s}\right)$ [Gillette, 1988].[2] Even a sparse vegetation cover with a fractional lateral cover (frontal silhouette area divided by ground area) greater about 2 to 4 percent can reduce the shear stress upon the surface to near zero under natural wind conditions [Marshall, 1971]. Nevertheless, there presumably exists an upper bound on U_* above which sweepup commences. This critical value likely depends not only on the type of plant and its stand density (plants per unit surface area), but also on the plant height, its water content, stem thickness, and aerodynamic cross section. However, for very dense plant covers such as small grains or grasses, we expect that the plants would either be lodged (i.e., knocked over), broken, or uprooted long before this critical shear stress is reached. The surface would no longer be as well protected and the critical shear velocity would drop to a value more representative of bare soils. (Similar modification would result if the plant cover were burned due to pre-shock thermal irradiation.) Unfortunately, no experimental data exists which relates high speed sweepup to shear stress over vegetated ground, although some measurements of the critical bending moment for wheat and barley stem breakage have been made [Oda, Suzuki, and Odagawa, 1966]. Lacking such data, we arbitrarily assume that a dense plant cover results in a threshold shear velocity of at least 3 m/s. Clearly, experiments must be performed to refine this value.

2.3 SEASONAL VARIATIONS.

All of the effects discussed above—the influence of vegetation cover, soil moisture, land use, and soil texture—imply that the potential for sweepup (and thus U_{*th}) must vary seasonally. Figure 1, derived from a database used to predict soil erosion in U.S. agricultural areas [Gillette and Passi, 1988], illustrates the expected variation U_{*th} for

2. One exception occurs when a planted field lies immediately downwind from a barren, sandy (low U_{*th}) surface from which sweepup is occurring. Material from the upwind source can then spread into the field, effectively "sandblasting" the plants and the underlying ground surface, thus initiating sweepup from where it would otherwise not be expected [Gillette, 1988]. Obviously, such downwind sandblasting effect could also be important in target areas containing a mixture of vegetated and bare (e.g., fallow) surfaces.

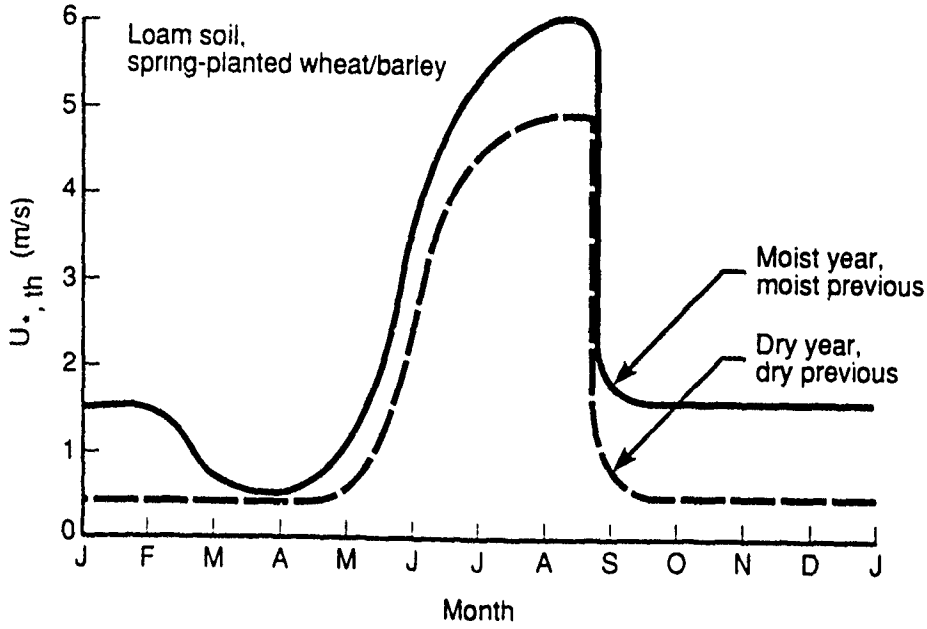

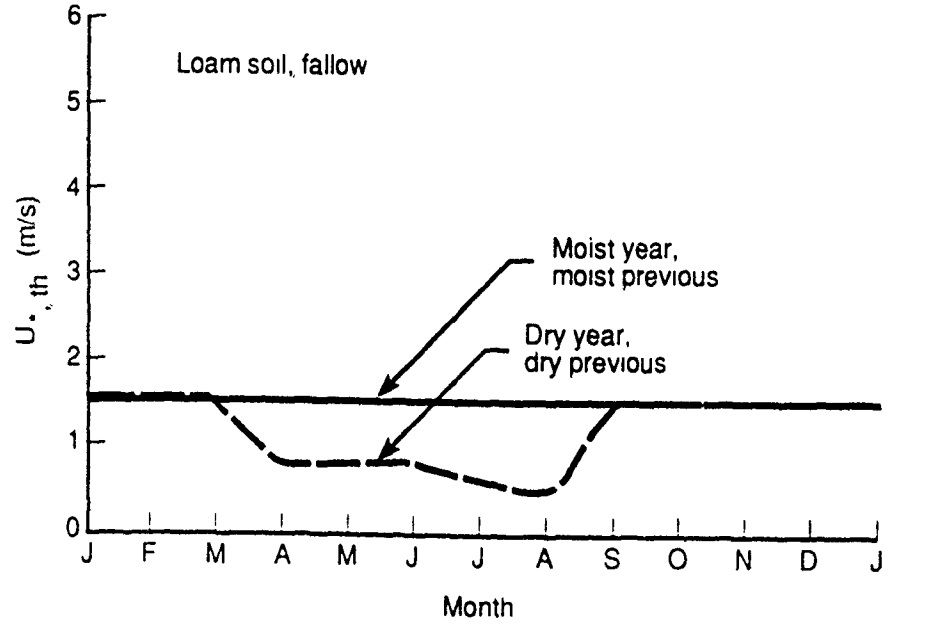

Figure 1. Threshold shear velocity as function of season for U.S. agricultural area—loam soil.

loam soil as function of time of year for two land use types (fallow land and a spring-planted crop) and for two "climatic" classes (corresponding to a prolonged moist period and a prolonged drought, respectively). A similar plot for sandy soil is shown in Fig. 2. Obviously, the most important influence is the presence and maturity of the crop (in this case, assumed to be a small grain cereal), which greatly increases the stability of the soil from shortly after germination in the spring until harvest in late summer. On the other hand, in spring, when the ground is plowed, crusts and clods are broken, the threshold velocity is reduced, and the soil becomes more vulnerable to wind erosion. After harvest, threshold velocities remain moderately high due to the common practice of leaving a vegetative residue or stubble through the winter. In drought years, however, insufficient moisture is available to support this residue and clodding and crusting of the surface is inhibited. Threshold velocities therefore remain low.

2.4 NUCLEAR INFLUENCES.

Threshold velocity measurements to date have focused only on conditions likely to be encountered under normal conditions. In a nuclear environment, however, several other factors may prove to have a crucial influence upon sweepup. For example, thermal radiation incident upon the surface prior to arrival of the blast wave can heat the soil to a point where bound water is explosively released, thus causing "popcorning" of particles from the surface [Versteegen, Rault, and Hillendahl, 1989]. This effect, which is most prevalent for clay soils, may disrupt surface crusts and lower the threshold velocity of the soil. On the other hand, thermal irradiation can also melt or "glaze" the surface, thereby stabilizing the soil by leaving a thin but presumably strong crust. Sandy surfaces are probably the most susceptible to glazing, although it has only rarely been observed, most notably following the TRINITY test in 1945 [P. Versteegen, personal communication, 1989].

Blast effects can also modify the dust producing potential of the surface. Airblast loading of subsurface air pores can cause spalling and disruption of an unbroken surface with the passage of the blast wave. The blast can also uproot trees and bushes, which would break the surface and reduce the threshold velocity, as well as increasing the shear stress upon the ground. Models relating blast effects to tree blowdown do exist [Morris, 1973]; however, no quantification of its effect upon soil lofting is yet available.

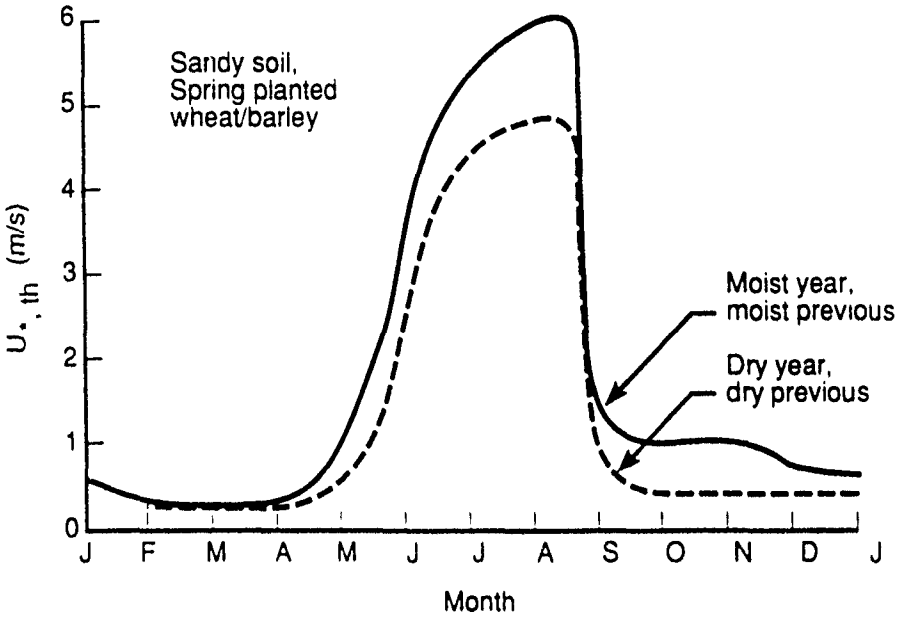

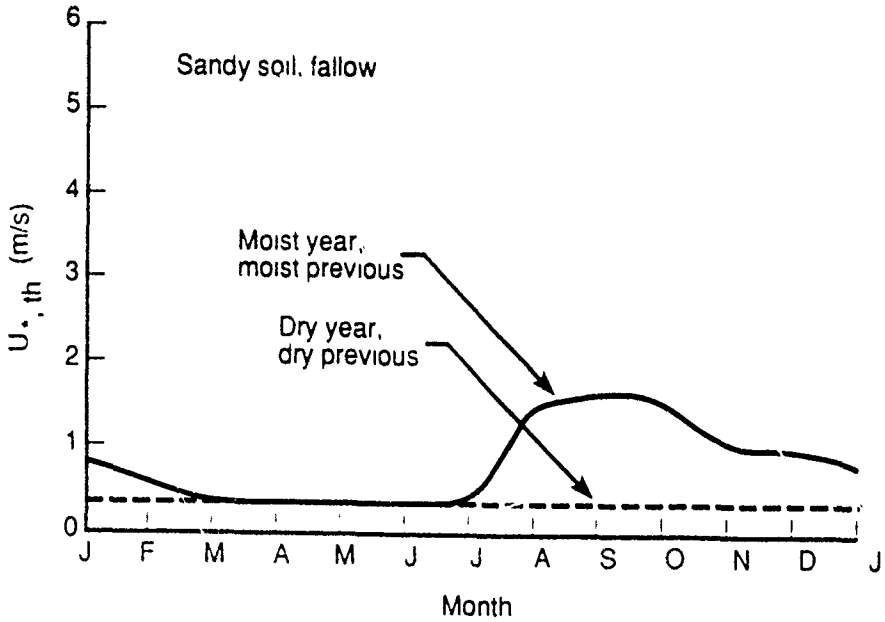

Figure 2. Threshold shear velocity as function of season for U.S. agricultural area—sandy soil.

SECTION 3

SWEEPUP MODEL

In the previous section, we reviewed many of the links between surface conditions and the *potential* for dust lofting. A general model would account for soil type, texture, moisture, temperature and vegetation. In this first analysis we roughly account for all parameters using a single quantitative measure—the threshold shear velocity. The sweepup model we develop is clearly an approximation, but nonetheless accounts for real soils in calculating the *amount* of dust leaving the surface.

3.1 BACKGROUND.

Sweepup models relate the vertical mass flux F of dust particles leaving the surface to the shear stress $\tau_* = \rho\ U_*^{\ 2}$ exerted on the ground by a sheared (rotational) wind field. The general form is

$$F = \alpha \left(U_* - U_{*th}\right)^{\beta} \qquad (3)$$

where $U_* > U_{*th}$ and α and β are empirical coefficients. At low wind speeds, dimensional analysis suggests that F should vary with the kinetic energy delivered to the surface [Gillette, 1980]. Thus we expect $\beta \approx 3$; this dependence has indeed been borne out by observations of natural sweepup from desert surfaces [Shinn et al., 1976; Westphal, Toon, and Carlson, 1987]. However, as wind speeds rise and dust concentrations increase, the lofted particles begin to act as a momentum sink on the airflow. Thus the shear on the surface is reduced, the lofting ability of the wind diminished, and F is no longer proportional to U_*^3. Unfortunately, there are very few measurements of F in this regime, especially at the very high wind speeds characteristic of nuclear blast waves. In one experiment [Hartenbaum, 1971], a value $\beta \approx 1.0$ was found over an uncohesive sand (mean particle radius 125 μm; $U_{*th} \approx 0.35$ m/s) surface for free stream wind speeds U between 34 and 115 m/s (corresponding to shear velocities in the range $5.0 \leq U_* \leq 18.6$ m/s). This result cannot be easily explained by simple dimensional analyses. A model which accounts for the effect of dust loading on the airstream at very high wind speeds is required.

3.2 HIGH SPEED MASS FLUX MODEL.

For wind speeds in the regime $U_* \gtrsim 10\ U_{*th}$, the vertical mass flux is related to the surface shear stress by (Mirels, 1984):

$$F = \rho_0 U_*^{\ 2}\ \frac{\ell n(1+B)}{U_0} \qquad (4)$$

where ρ_0 and U_0 are the density and horizontal wind velocity in the free stream (i.e., at the top of the dusty surface layer) and B is a dimensionless *blowing parameter* which expresses the effect of transverse particle injection on the local shear stress in plane parallel flow. Assuming that the mass loading effectively reduces the shear stress to the threshold value required to maintain dust lofting, B is given by the implicit relation

$$\ell n(1+B) = B\left[\frac{U_*}{U_{*th}}\right]^2 , \qquad (5)$$

which, in the suspension regime ($U_* \gtrsim 10\ U_{*th}$), can be approximated

$$\ln(1 + B) \approx 3.92 \left[\frac{U_*}{U_{*th}} \right]^{0.24} \quad . \qquad (6)$$

The functional dependence of B on the shear stress ratio τ_*/τ_{*th} given by Eqs. (5) and (6) is illustrated in Fig. 3.

To prescribe U_0 as a function of time, ground range, yield, and height of burst, we use the ideal airblast approximations given by Brode (1987). These approximations are valid only during the positive overpressure phase of the blast; we therefore assume all the sweepup occurs during the positive phase. The free-stream velocities are then used to compute the shear velocity U_* according to the "rough plate" formula [Schlichting, 1958]:

$$U_* = \frac{U_0}{\sqrt{2}} [2.87 + 1.58 \log(x/K_s)]^{-1.25} \quad , \qquad (7)$$

where x is the distance behind the shock wave, $K_s \sim 0.05$ m is the roughness height, and $x > 100\ K_s$. Finally, substituting Eqs. (6) and (7) into Eq. (4), we obtain [see Eq. (8) below]

The sweepup mass flux is therefore inversely (but weakly) dependent upon threshold velocity. This expression compares well with the experimental result $F \propto U_0^{1.144}$ derived by Hartenbaum [1971] and subsequently used as the basis for many nuclear sweepup models [Schlamp, Schuckman, and Rosenblatt, 1982; Bacon, Dunn, and Sarma, 1988]. However, unlike previous models, the dependence of sweepup on threshold velocity (and hence on surface type) is *explicit* in Eq. (8).

$$\boxed{F \approx \frac{1.80\ \rho_0}{U_{*th}^{0.24} [2.87 + 1.58 \log(x/K_s)]^{2.80}} U_0^{\ 1.24} \quad . \qquad (8)}$$

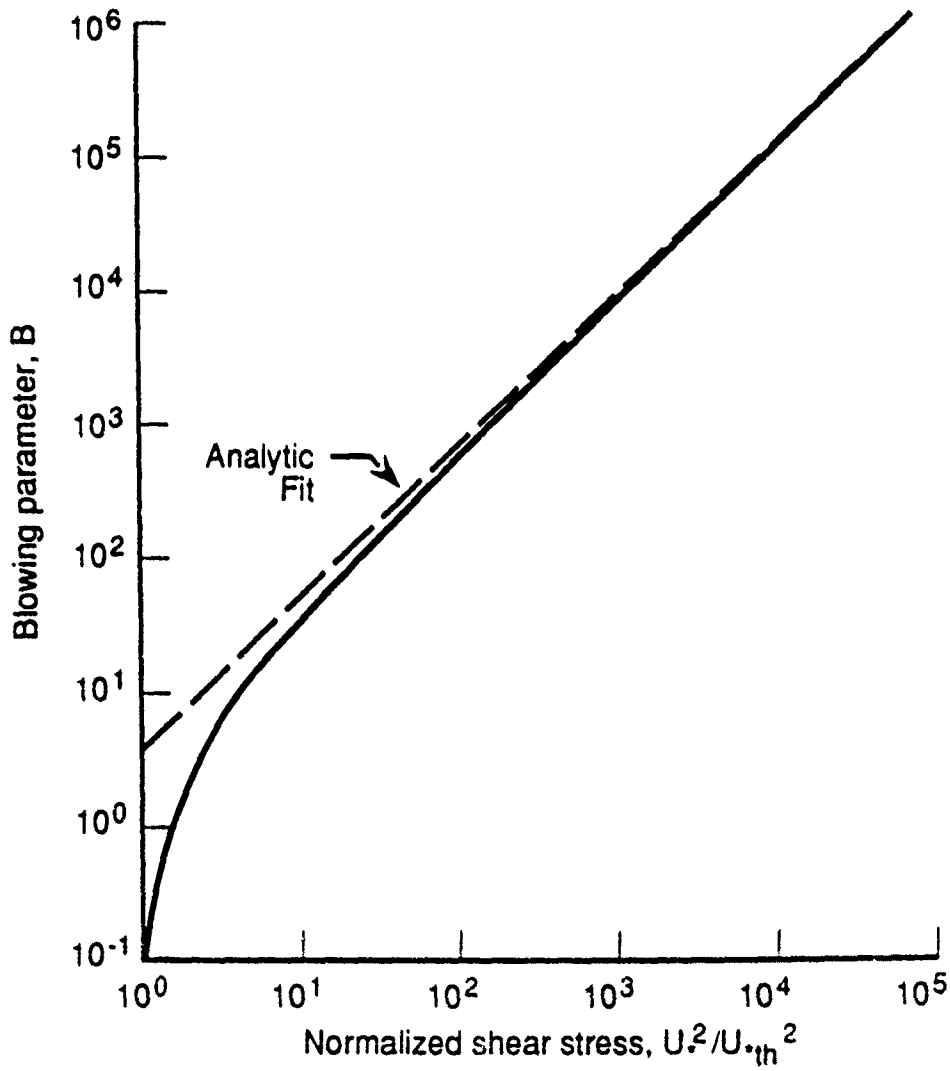

Figure 3. Blowing parameter as function of normalized shear stress.

SECTION 4

SWEEPUP CALCULATIONS

We now use the mass flux model and ideal blast wave driver to compute the variation in net sweepup as a function of threshold shear velocity. Two quantities are of interest: (1) The integrated sweepup mass M; and (2) the *effective sweepup radius* R_E, defined as the the maximum range (from ground zero) at which sweepup can occur for a given yield, HOB, and surface type.

4.1 METHODOLOGY.

We treat the surface as flat, homogeneous (i.e., no spatial variations in threshold velocity), and thermally ideal. Assuming cylindrical symmetry about the burst point, the incremental dust mass ΔM_i lofted from a ring of width ΔR and radius R_i is

$$\Delta M_i = 2\pi\ R_i \Delta R \int_T^{T+D_u} F_i dt \qquad (9)$$

where T is the blast wave time of arrival at R_i, D_u is the dynamic pressure positive phase duration, and F_i is the local sweepup mass flux (Eq. 8). We set $\Delta R_i \approx$ 60 m and use empirical formulae to determine T and D_u as functions of height of burst, yield, and range [Brode, 1987]. To simulate the low windspeed cutoff for dust suspension, we further assume F_i = 0 for $U_* < 10\,U_{*th}$.

Equation (9) is integrated numerically using the trapezoidal rule and a timestep $\Delta t = D_u/100$ for i = 1 to i = IMAX, where IMAX corresponds to the first ring where no sweepup occurs ($\Delta M_{IMAX} = 0$). Thus $R_{IMAX-1} = R_E$ defines the effective sweepup radius. The total sweepup mass M is then found by simply summing over the rings:

$$M = \sum_{i=1}^{IMAX} \Delta M_i \quad . \qquad (10)$$

Note that M is a measure of the *initial* sweepup; it does not account for mass fallback to the surface, nor does it include mass lofted during the negative phase.

4.2 VARIATIONS IN SWEEPUP MASS.

We have computed the variation in total sweepup mass M for threshold shear velocities from 0.20 to 4.0 m/s, scaled heights of burst (SHOBs) from 20 to 1000 ft/KT$^{1/3}$, and yields (W) from 500 to 1000 KT.[3] Figure 4 shows the dependence of M on U_{*th} for a 500 KT detonation at three burst altitudes: 397 ft (SHOB = 50 ft/KT$^{1/3}$), 1984 ft (SHOB = 250 ft/KT$^{1/3}$), and 3969 ft (SHOB = 500 ft/KT$^{1/3}$). We find that M decays exponentially with increasing U_{*th}, and is most sensitive to variations in threshold velocity at low U_{*th}—i.e., over dry, loose, unvegetated soils. In this regime, small changes in surface type can produce large changes in sweepup. For example, we find that a 50 ft SHOB detonation over loose sand (U_{*th} = 0.28 m/s) raises over two times as much mass as an

3. The burst altitude SHOB = 20 ft/KT$^{1/3}$ roughly corresponds to the minimum for non-cratering airbursts [Rosenblatt, 1981].

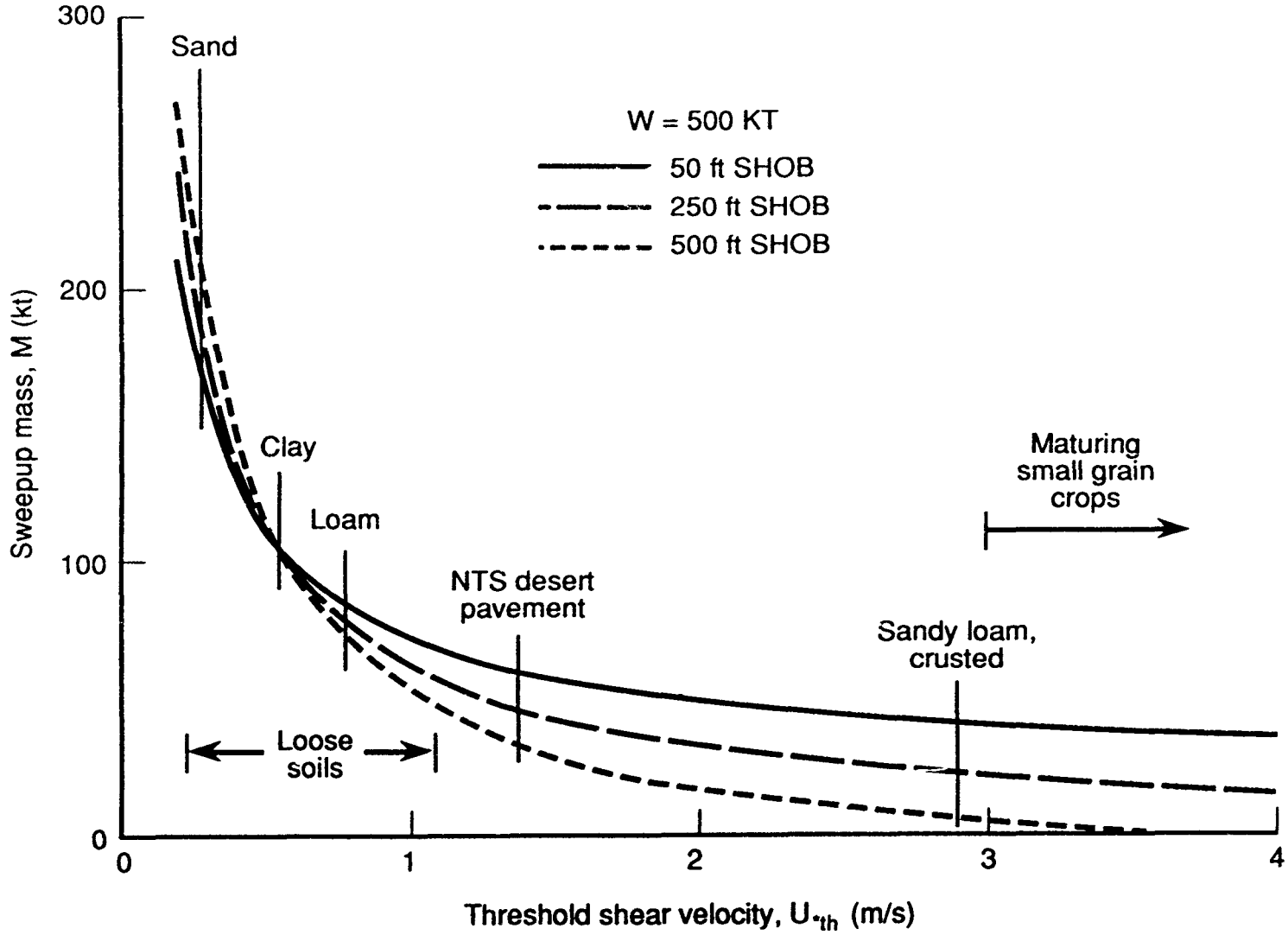

Figure 4. Net sweepup mass as function of threshold shear velocity.

identical burst over loose loam (U_{*th} = 0.78 m/s). If the burst occurs at an even higher altitude (e.g., 500 ft SHOB), the difference is more pronounced. For highly non-erodible soils ($U_{*th} \gtrsim 2.0$) or soils which are densely vegetated ($U_{*th} \gtrsim 3.0$), sweepup is strongly suppressed, especially at higher burst altitudes. Indeed, we find that when a 500 ft SHOB detonation occurs over a surface with $U_{*th} > 3.5$ m/s (characteristic of an early to mid-summer wheat crop—see Figs. 1 and 2), no sweepup occurs at all.

The strong dependence of sweepup mass on burst altitude is illustrated in Fig. 5. Here we have plotted M as a function of SHOB for a 500 KT burst over four surface types ranging from loose sand to a desert pebble pavement (mass equivalent modal pebble diameter 1.0 cm) similar to that found in Yucca Valley at the Nevada Test Site (NTS). We find that the dependence of M on SHOB is highly nonlinear, with the largest variations occurring over the most erodible soils. In particular, we find that sweepup mass at first decays rapidly with increasing SHOB, reaching a relative minimum around 80 to 100 ft SHOB. With further increases in burst altitude, however, the sweepup mass begins to rise—indicative of the build-up in blast dynamic pressure with increasing SHOB for shocks waves in the Mach reflection regime. The positive dependence of M on SHOB continues until an altitude is reached at which the Mach wave begins to weaken—typically between 300 and 400 ft SHOB. For bursts above this altitude, sweepup again diminishes, eventually dropping to zero. Over desert pavement, the cutoff occurs at SHOB = 760 ft/KT$^{1/3}$ (HOB = 6032 ft); over loam, it is at SHOB = 935 ft/KT$^{1/3}$ (HOB = 7421 ft). These results are modified somewhat over non-ideal surfaces due to enhanced velocities in the precursed wave. In particular, M is increased relative to the results in Fig. 5 for all SHOB $\lesssim$ 650 ft/KT$^{1/3}$.

Sweepup also increases with yield. Figure 6 shows the variation in M for four surface types and two burst altitudes (50 and 250 ft SHOB) for yields between 500 KT and 1 MT. The calculations show a linear dependence on yield in this range, with sandy surfaces being the most sensitive to changes in W and desert pavement the least. Thus the *sweepup efficiency* (defined as soil mass lofted per megaton of weapon yield) is yield dependent. For example, a 500 KT burst at 50 ft SHOB produces sweepup efficiencies ranging from 0.12 Tg/MT for desert pavement to 0.33 Tg/MT for sand. Raising the yield to 1 MT, however, nearly doubles these values to between 0.23 and 0.64 Tg/MT. Slightly lower efficiencies result at all yields when the burst occurs at a higher altitude (250 ft SHOB) over the two least erodible surfaces (loam and desert pavement), while higher efficiencies are obtained over the most erodible ones. This is consistent with Fig. 5.

4.3 VARIATIONS IN SWEEPUP RADIUS.

The variations in sweepup mass discussed above can be attributed to a combination of two factors: (1) Variations in positive-phase dynamic impulse integrated over the sweepup area, and (2) variations in the size of the sweepup area itself. Sweepup area can be characterized by the effective sweepup radius R_E. Figure 7 shows the dependence of R_E on threshold shear velocity for three burst altitudes. Comparing these results with Fig. 4, it is clear that the sweepup mass M depends strongly upon R_E—both decay exponentially with increasing U_{*th}, and both display the greatest sensitivity to threshold velocity over bare, loose soil. (Not all the dust to radius R_E is lofted to stabilization; but all is raised from the surface and is directed toward the

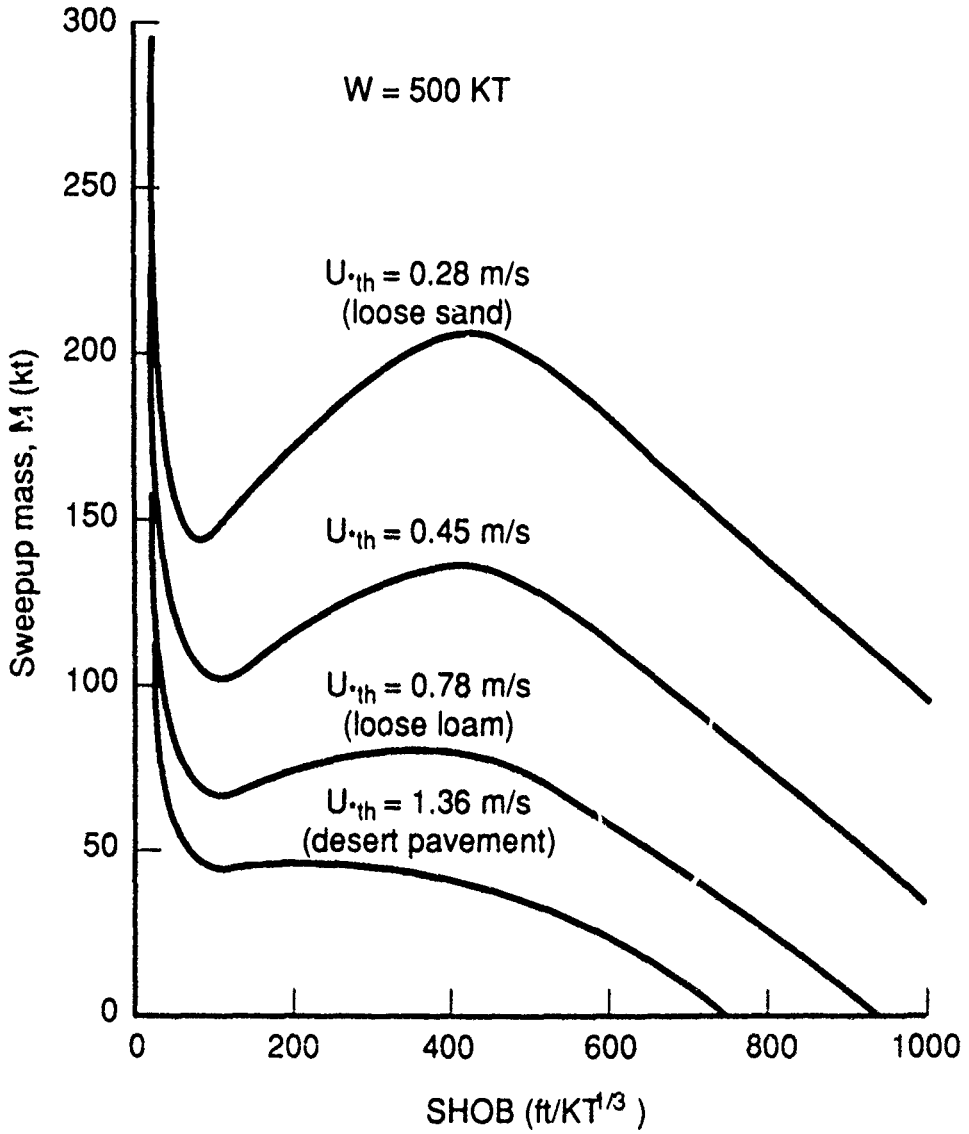

Figure 5. Net sweepup mass as function of burst altitude.

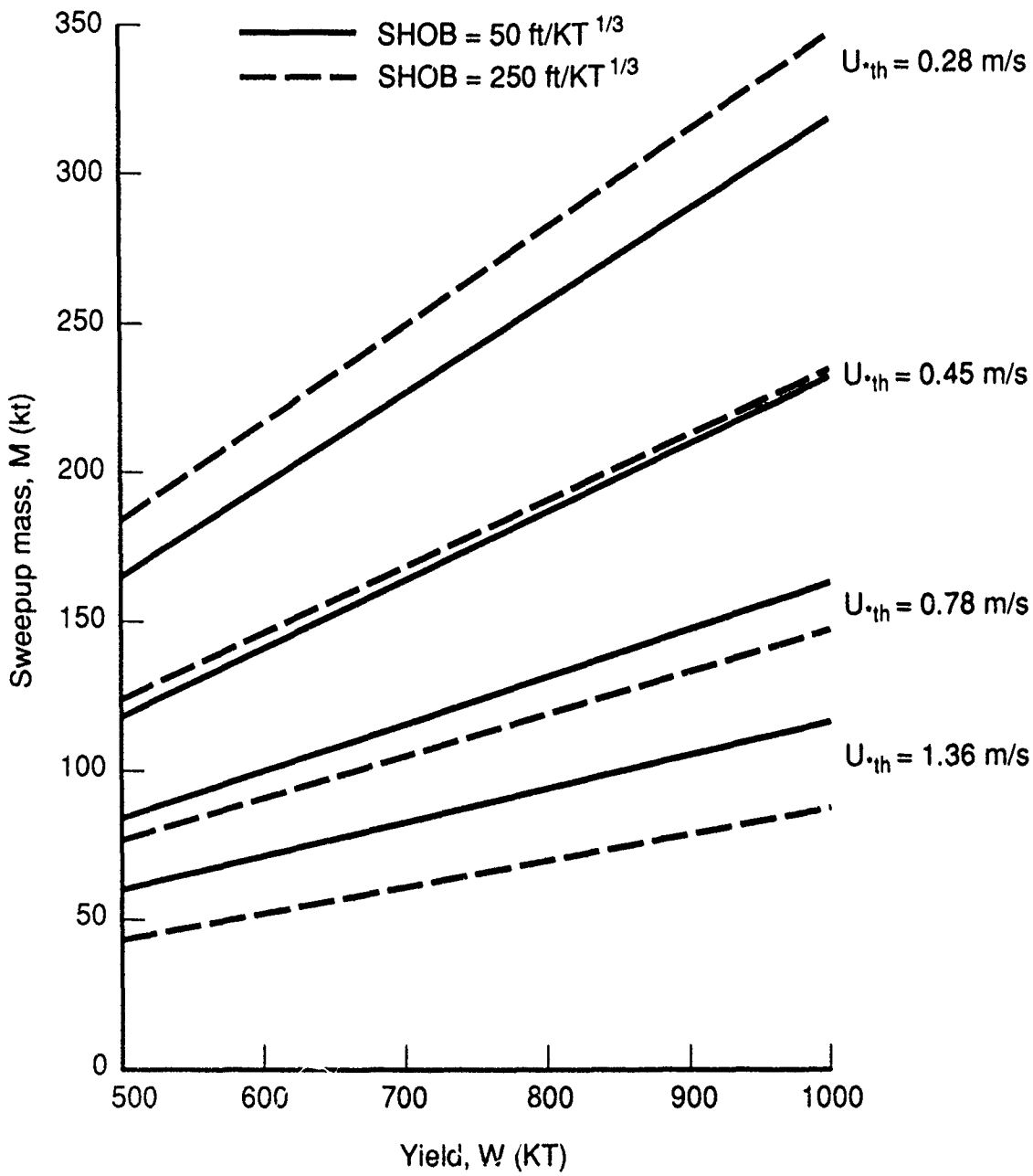

Figure 6. Net sweepup mass as function of yield.

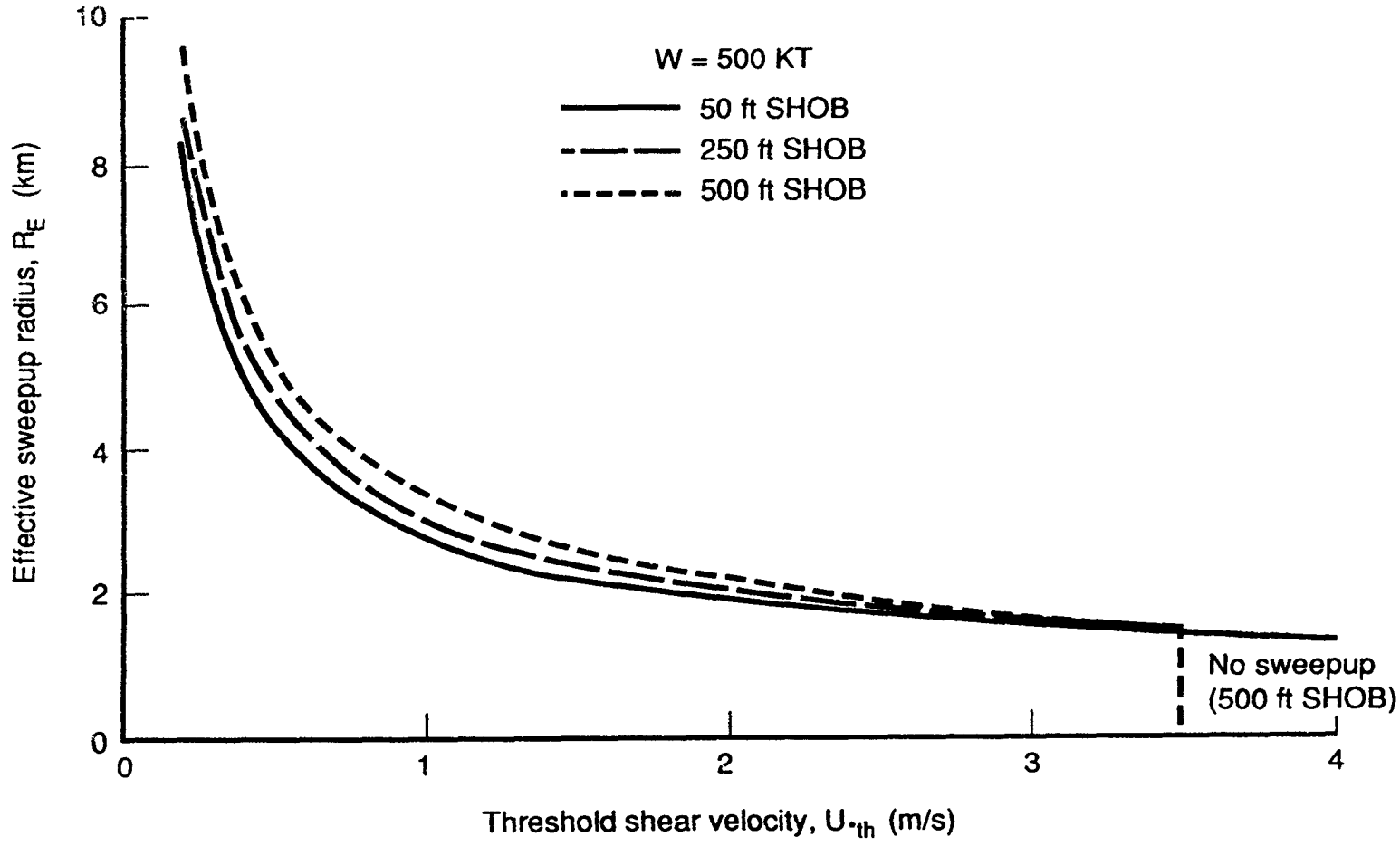

Figure 7. Effective sweepup radius as function of threshold shear velocity.

pedestal.) Unlike the sweepup mass, however, there is no "crossover" with increasing threshold velocity; the sweepup radius for a 500 ft SHOB burst is *always* larger than for detonations at lower altitudes (at least until the cutoff at U_{*th} = 3.5 m/s is reached). This is as we would expect for a Mach reflected shock. It simply indicates that as bursts occur at greater heights above the surface, more of the kinetic energy is converted into horizontal dynamic pressure. The relationship between R_E on SHOB is illustrated in more detail in Fig. 8. Unlike the sweepup mass M (Fig. 5), we find that R_E varies linearly with SHOB.

Finally, in Fig. 9, we show the variation in R_E as a function of yield. Again, the dependence is linear, with the greatest sensitivity found for the most erodible soils. However, when expressed in terms of sweepup area $\left(\pi R_E^2\right)$, this sensitivity disappears. For example, from Fig. 9, we find that a 1-MT burst always sweeps an area about 1.6 times larger than a 500-KT detonation at the same altitude, regardless of soil type.

4.4 NEVADA TEST SITE SOIL.

All of the results presented so far have implicitly assumed that the soil properties are independent of depth. Thus we have assumed that the threshold shear velocity remains constant throughout the period sweepup is occurring. For many agricultural soils, which have a deep, well-mixed upper layer of topsoil, this is an appropriate assumption. But many natural soils are not so homogeneously structured. The Yucca Valley region of the NTS is an example. Soils in most of this area are representative of "wind-stabilized" alluvium from which most of the erodible (i.e., small) surface elements have long since been removed by natural wind processes. As a result, the soil has a two-layer structure: A thin desert pavement veneer consisting of large pebbles (tens of millimeters to a centimeter or two in diameter), overlying a deeper layer of finer material—typically sand or sandy loam imbedded with gravel. This desert pavement is usually sufficient to prevent wind erosion of the fine particles for all but the strongest *natural* winds; in a nuclear environment, however, it is easily removed, as has been observed following bursts over Yucca Valley [Lamar, 1962]. It therefore seems likely that nuclear sweepup over desert pavements may proceed in two stages: A first stage during which only the large particles comprising the top layer layer are removed, followed by second, more vigorous stage during which the now-exposed underlying soil is scoured. Thus, more mass may ultimately be lofted than if only the heavy top layer were present.

To test whether this two-stage process can significantly increase the net sweepup mass, we have modified our model to account for the presence of desert pavement over a fine soil. We assume that the surface is initially covered with a single layer of pebbles with mass modal diameters D_m = 1 cm. To this layer we assign a threshold shear velocity U_{*th} = 1.36 m/s. This value is consistent with the empirical relation for dry, disturbed desert soils [Gillette et al., 1980]

$$U_{*th} = 0.43 + 0.93\ D_m \qquad (11)$$

where D_m is in centimeters. Assuming the particles are spherical and have a mass density 2.0×10^3 kg/m^3, we calculate the areal density of the pebble layer to be $10.5\ A_p$ kg/m^2, where $0 < A_p \leq 1.0$ is the area fraction of ground actually covered by pebbles. (We estimate $A_p \sim 0.3$ for Yucca Valley.) Setting U_{*th} = 1.36 m/s in Eq. 8 and using Eq. 9, the time-dependent pebble mass removed from each concentric ring around ground zero

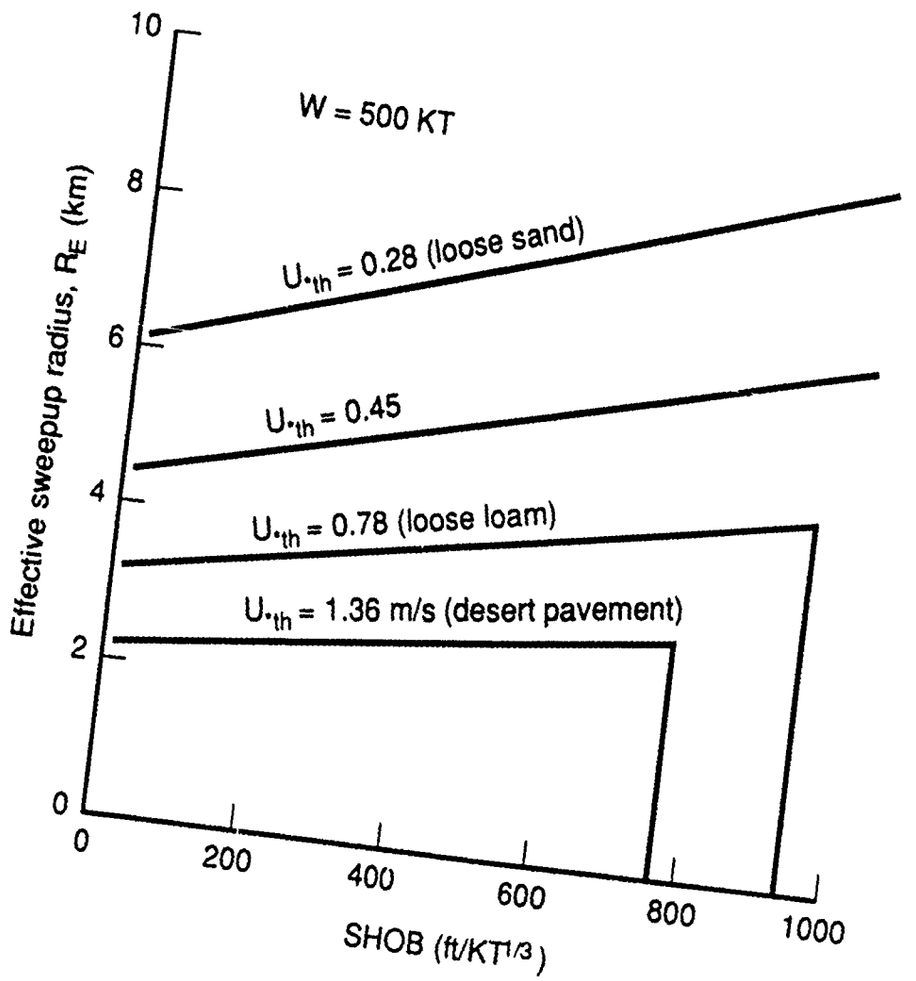

Figure 8. Effective sweepup radius as function of burst altitude.

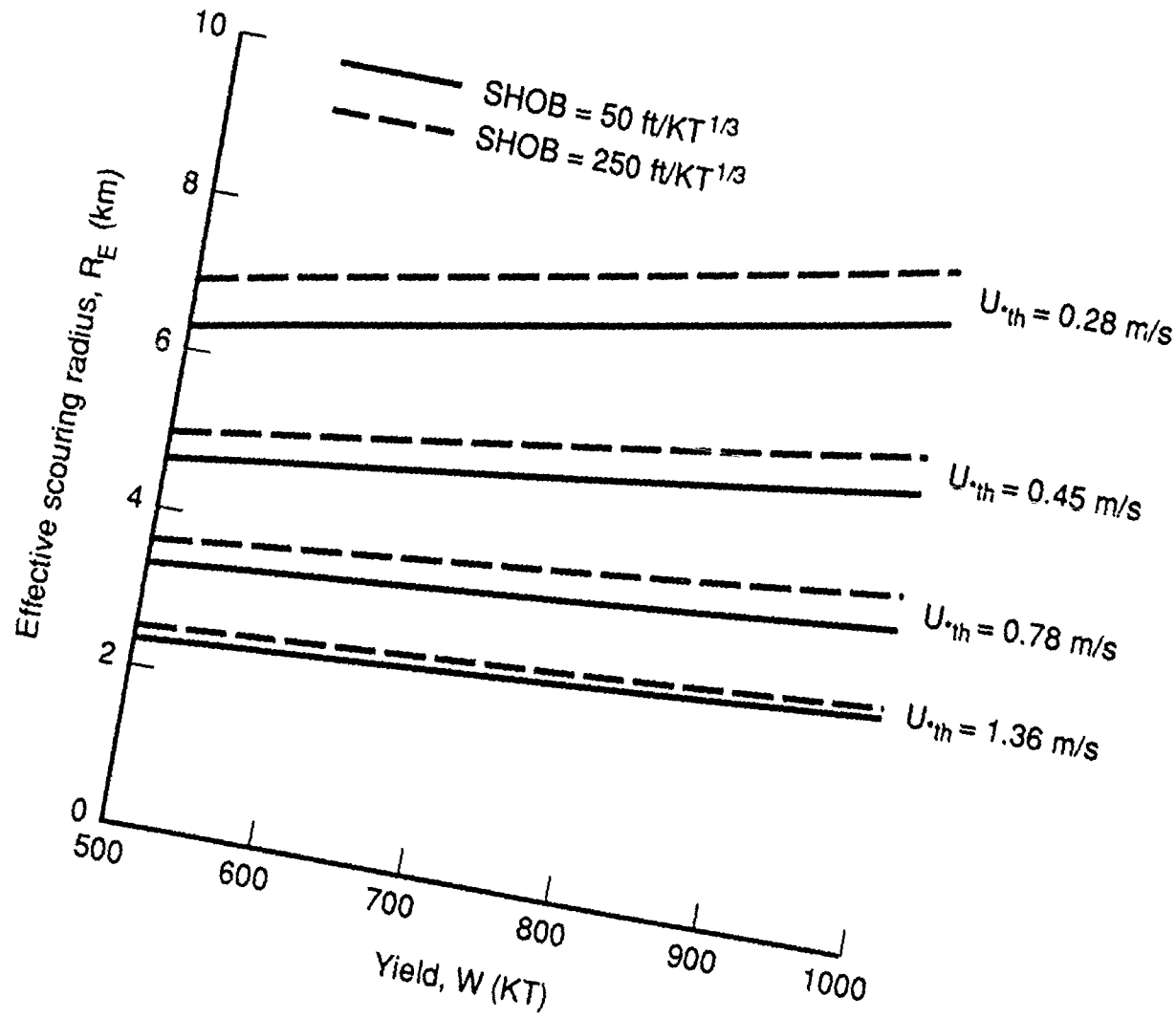

Figure 9. Effective sweepup radius as function of yield.

is calculated. If, before the sweepup phase ends, we find the total mass removed has exceeded the critical density 10.5 A_p kg/m^2, we assume that the pebble layer has been completely removed from that ring. We then "instantaneously" reset U_{*th} to a lower value to simulate the exposure of the underlying fine particles, and proceed with the calculation until sweepup ends.

We have computed the net sweepup mass for a 50 ft SHOB burst at two yields (500 and 1000 KT) over three different desert pavement configurations: (1) A single pebble veneer over highly erodible sand (U_{*th} = 0.28 m/s), (2) a single pebble veneer over an intermediately erodible soil (U_{*th} = 0.45 m/s), and (3) an "infinitely deep" pebble layer for which U_{*th} remains fixed at 1.36 m/s throughout the calculation. The results are presented in Table 2. We find desert pavement to be surprisingly more stabilizing than expected. Only when the pavement overlies loose sand and is sparsely distributed (A_p = 0.3) do we find an enhancement in sweepup mass in excess of 10 percent. This is in spite of the fact that we compute complete removal of the pebble veneer (for A_p = 0.3) out to approximately 425 ft/KT$^{1/3}$ range (≈ 1.4 km for a 1-MT burst). This is equivalent to nearly one-quarter the entire sweepup area. However, the most significant scouring of the underlying soil is restricted to ranges much closer to ground zero; thus the net sweepup mass is proportionately reduced.

Table 2. Sensitivity of sweepup mass to desert pavement cover for 50 ft SHOB burst.

Threshold Shear Velocity of Underlying Soil (m/s)	Yield, W (KT)	Areal Pebble Cover, A_p	Sweepup Mass, M (kt) Pebbles Only	Sweepup Mass, M (kt) Pebbles Overlying Fine Soil	Difference (%)
0.28	500	0.3	60.09	65.77	+9.42
		0.5	60.09	63.67	+5.92
		1.0	60.09	62.31	+3.66
	1000	0.3	117.20	130.30	+11.18
		0.5	117.20	125.70	+7.25
		1.0	117.20	122.40	+4.44
0.45	500	0.3	60.09	63.90	+6. 34
		0.5	60.09	62.36	+3.78
		1.0	60.09	60.10	+0.02
	1000	0.3	117.20	126.20	+7.68
		0.5	117.20	122.70	+4.69
		1.0	117.20	120.40	+2.73

These results would be drastically different for non-ideal surfaces when thermal layers and precursors are accounted for. The resultant elevated dynamic pressures would likely remove the pebble veneer much sooner and to a greater distance from ground zero. The net sweepup mass would therefore be higher. This is partially supported by the observation of Lamar (1962), who found near complete removal of the desert pavement out to at least 600 ft/KT$^{1/3}$ from ground zero following shot SHASTA (W = 16.5 KT, SHOB = 196 ft/KT$^{1/3}$) in Yucca Valley. Separate evidence, however, indicates that this shot did not produce a strong precursor [Liner et al., 1975].

4.5 NORMALIZED SWEEPUP MASS.

Figure 10 shows the variation in sweepup mass as a function of threshold velocity normalized by that calculated for Yucca Valley, NTS. To compute the normalization factor M_{NTS}, we adopted the "two-layer" model described above with $A_p = 0.3$ and $U_{*th} = 0.45$ m/s for the underlying soil; the results are indicated in the figure. (Our choice $U_{*th} = 0.45$ m/s is somewhat arbitrary; it probably underestimates the dust pickup at the NTS since some of the desert pavement was broken by pre-shot construction and traffic.) These results emphasize that, compared to most dry barren or semi-barren dry surfaces, Yucca Valley soil is not as readily eroded. This is due to the stabilizing effect of the desert pavement pebble cover. Most other bare soils—for example, agricultural soils during a dry winter or immediately after plowing or harvest—actually produces *more* sweepup than the Yucca Valley surface. For example, for detonations at 50 to 500 ft SHOB over bare loam surfaces (U_{*th} = 0.78 m/s), between 1.3 and 2.2 times more dust would be raised. On the other hand, if the surface were heavily vegetated (U_{*th} > 3.5 m/s), the sweepup is reduced to anywhere from zero to about 50 percent of its NTS mass.

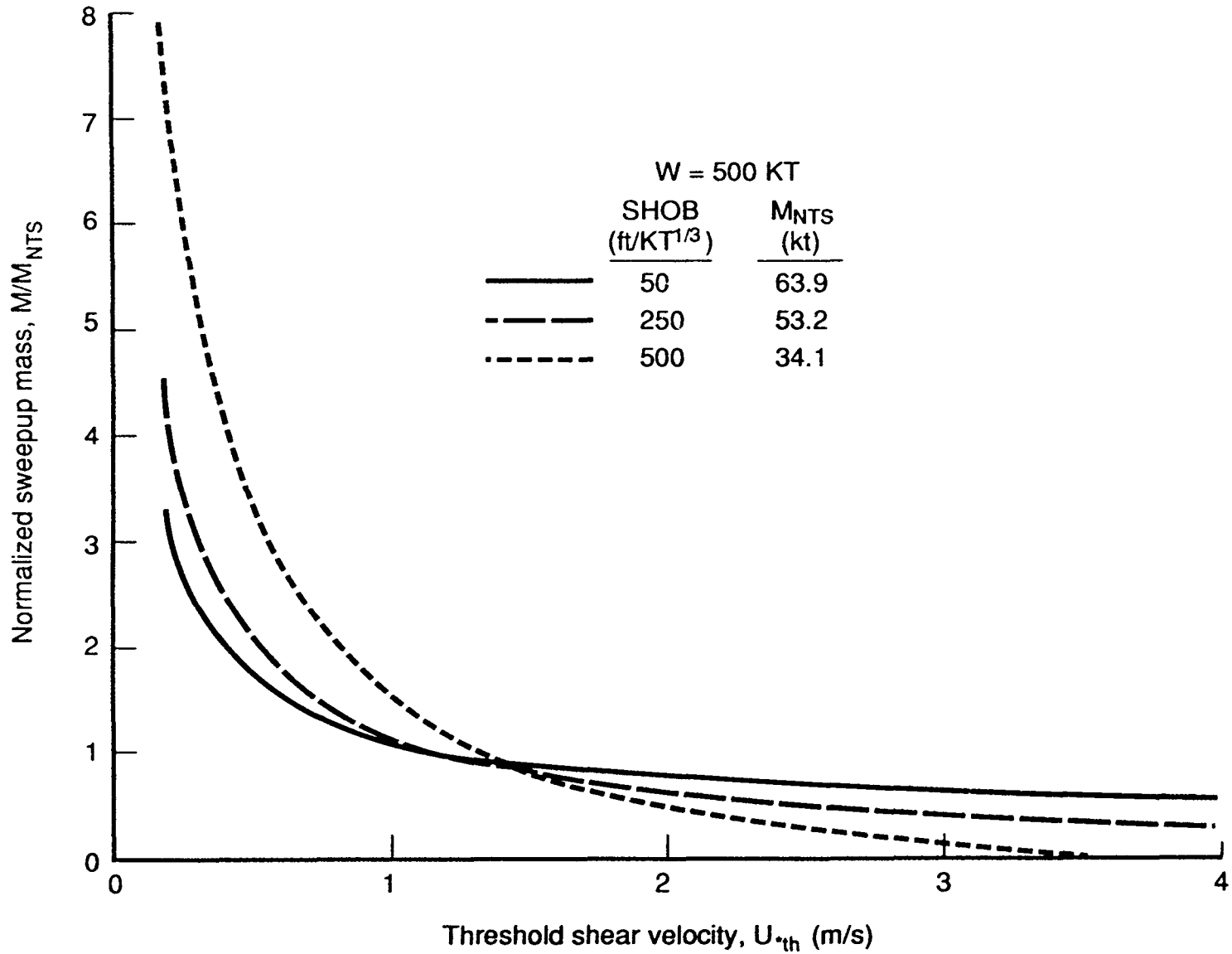

Figure 10. Sweepup mass relative to airburst over Yucca Valley as function of threshold shear velocity.

SECTION 5

IMPLICATIONS FOR TARGET AREAS

Surfaces in target areas vary widely reflecting differences in soil type, topography, moisture levels, and vegetation cover. Most real target surfaces do not resemble the Nevada desert, nor do they remain invariant throughout the year. Small differences in surface properties can lead to large changes in dust sweepup.

The real soil sweepup model we developed used a single parameter, the threshold velocity, to account for soil type, moisture, and vegetation cover. Clearly this is a simplification, but one that nonetheless accounts for experimental data on low-speed scouring of real soils. In extending this analysis to nuclear sweepup, we recognize that several potentially important physical processes are treated inadequately or not at all. Inclusion of (a) non-ideal shock effects, (b) blast and thermal modification of surface properties, (c) uneven terrain effects, and (d) post-positive phase blast winds would no doubt alter the results somewhat. We anticipate that each of these processes modifies the real soil corrections we calculate, nevertheless, the conclusions indicate:

- Targets located on cropland have the greatest dust producing potential, since the surface tends to be bare at least part of the year—especially during the spring plowing and immediately after harvest in the autumn (Figs. 1 and 2). Moreover, some portion of the land remains bare (i.e., fallow) all year around. For example, in U.S. target regions, typically one-fourth the area devoted to crops is fallow at any given time [North Dakota Agricultural Statistics Service, 1988].

- A crop or grass cover may be sufficient to completely suppress sweepup from a 500 KT airburst if the SHOB is greater than 500 ft/KT$^{1/3}$ (Fig. 4). Thus late summer is the least vulnerable time of year for sweepup; this is when crop and grass densities are greatest.

- There exists an optimum burst altitude between SHOB = 80 to 100 ft/KT$^{1/3}$ at which the sweepup mass is minimized over bare soils. Bursts detonated below this altitude or between 300 and 400 ft/KT$^{1/3}$ tend to maximize dust production (Fig. 5).

- For a fixed SHOB, sweepup mass tends to increase with increasing yield. The sensitivity to yield is greatest for the most erodible soils (Fig. 6).

- The effective sweepup radius increases with increasing burst altitude and yield, and is most sensitive to surface conditions over highly erodible soil (Figs. 7-9).

- Bare, dry agricultural soils (composed primarily of loam) produce up to 220 percent more sweepup mass than a desert pavement surface typical of the NTS (Fig. 10).

Our results also imply that sweepup may not be uniform even within a single target area. Intercontinental Ballistic Missile silo fields are quite large, typically covering an area on the order and 10^4 km^2 in the U.S. and somewhat less in the Soviet Union. Surface conditions within an area so large are not necessarily uniform. A burst over one portion of a silo field could yield a much different sweepup amount and scour an area considerably larger or smaller than a burst

in another portion of the field. Fratricide probabilities could thus be highly variable.

Figure 11 depicts a U.S. target area. Aside from isolated urban areas and bodies of water, most of the land shown here is either planted (primarily with wheat, oats, and barley) or is tall-grass wildland. Yet the soil upon which this vegetation grows is not the same across the entire region; roughly half the silos are located on loamy soil which is well-drained and hence dry (except for periods immediately after a rainfall or in irrigated zones). Thus, assuming U_{*th} = 0.78 m/s, our results indicate a maximum sweepup efficiency of about 0.16 Tg/MT for a 500-KT low altitude burst, ranging up to ≈ 0.30 Tg/MT for a 1-MT detonations. In addition, we calculate maximum sweepup radii between 3 and 4 km from the burst point—roughly one-third to one-half the mean spacing between silos. Smaller sweepup radii and lower efficiencies are to be expected from strikes against those silos located on moist or poorly drained soils, or following attacks during less vulnerable times of year such as summer or when the surface is snow-covered or frozen.

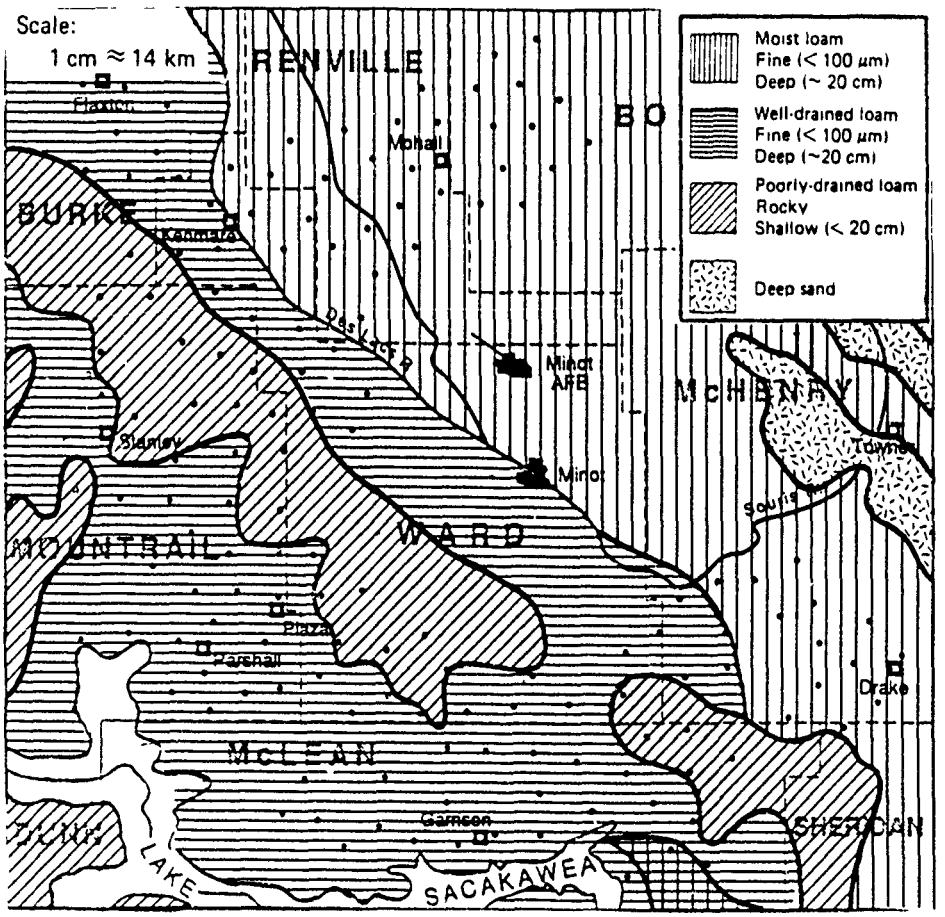

Source: Aandahl [1982]; Omodt et al. [1968].

Figure 11. Soils in the Minot AFB, North Dakota ICBM silo area (dots indicate silo locations).

SECTION 6

CONCLUSIONS

We find that the threshold shear velocity provides a useful quantitative measure of the susceptibility of a surface to nuclear sweepup. Wide variations in this parameter occur naturally with seasonal and regional differences in vegetation cover, soil moisture, soil type, and land use. We find that such variations can lead to large changes in the initial sweepup mass raised by a low altitude airburst—particularly over surfaces which are dry and minimally vegetated. When vegetation is present, the surface is strongly stabilized; in fact, a dense agricultural cover can in some cases completely suppress sweepup. By extrapolating our results to real soil conditions in target regions, we expect even larger variations in sweepup mass could result under attack conditions. We find that sweepup is minimal as long as the vegetation cover remains intact; at high overpressures or high thermal fluxes, the stabilizing influence is diminished. The threshold velocities at which plant lodging, breakage, and uprooting occur are not yet established, but it is nevertheless clear that sweepup is greatly reduced.

SECTION 7

LIST OF REFERENCES

Aandahl, A. M., *Soils of the Great Plains*, University of Nebraska Press, Omaha, Nebraska, 1982.

Alderfer, R. B., "Soil," *McGraw-Hill Encyclopedia of Science and Technology*, Vol. 12, McGraw-Hill, Inc., New York City, 1977.

Bacon, D. P., T. P. Dunn, and R. A. Sarma, *Late-Time Cloud Modeling, Vol. 1: Cases N1-N6*, Science Applications International Corporation, McLean, Virginia, SAIC-88/1856, 1988.

Bagnold, R. A., *The Physics of Blown Sand and Sand Dunes*, Methuen and Co., Ltd., London, 1941.

Brode, H. L., *Airblast from Nuclear Bursts—Analytic Approximations*, Pacific-Sierra Research Corporation, Los Angeles, California, PSR 1419-3, 1987.

Businger, J. A., "Turbulent Transfer in the Atmospheric Surface Layer," in D. A. Haugen (ed.), *Workshop on Micrometeorology*, American Meteorological Society, Boston, Massachusetts, 1973.

Chepil, W. S., "Influence of Moisture on Erodibility of Soil by Wind," *Soil Sci. Soc. Amer. Proc.*, Vol. 20, 1956, pp. 288-292.

Dorrance, W. H., *Viscous Hypersonic Flow*, McGraw-Hill, Inc., New York City, 1962.

Gillette, D. A., "Tests with a Portable Wind Tunnel for Determining Wind Erosion Threshold Velocities," *Atmos. Environ.*, Vol. 12, 1978, pp. 2309-2313.

Gillette, D. A., "Major Contributions of Natural Primary Continental Aerosols: Source Mechanisms," in T. J. Kneip and P. J. Lioy (eds.), *Aerosols: Anthropogenic and Natural, Sources and Transport*, New York Academy of Sciences, New York City, 1980.

Gillette, D. A., "Threshold Friction Velocities for Dust Production for Agricultural Soils," *J. Geopyhs. Res.*, Vol. 93, 1988, pp. 12645-12662.

Gillette, D. A., et al., "Threshold Velocities for Input of Soil Particles into the Air by Desert Soils," *J. Geophys. Res.*, Vol. 85, 1980, pp. 5621-5630.

Gillette, D. A., et al., "Threshold Friction Velocities and Rupture Moduli for Crusted Desert Soils for the Input of Soil Particles into the Air," *J. Geophys. Res.*, Vol. 87, 1982, pp. 9003-9015.

Gillette, D. A. and K. J. Hanson, "Spatial and Temporal Variability of Dust Production Caused by Wind Erosion in the United States," *J. Geophys. Res.*, Vol. 94, 1989, pp. 2197-2206.

Gillette, D. A. and R. Passi, "Modeling Dust Emission Caused by Wind Erosion," *J. Geophys. Res.*, Vol. 93, 1988, pp. 14233-14242.

Glasstone, S. and P. J. Dolan, *The Effects of Nuclear Weapons*, Third Edition, United States Department of Defense and Energy Research and Development Administration, Washington, D.C., 1977.

Hartenbaum, B., *Lofting of Particulates by a High Speed Wind*, Defense Nuclear Agency, Washington, DC, DNA 2737F, 1971.

Lamar, D. L., *Preliminary Study of the Distribution of Desert Pavement in Relation to Blast Areas at the Nevada Proving Grounds*, RAND Corporation, Santa Monica, California, Report D-10270-PR, 1962.

Liner, R. T., et al., *Nuclear Precursor Phenomenology and Sweep-Up Dust Cloud Model Development*, Defense Nuclear Agency, Washington, DC, DNA 3781F, 1975.

Marshall, J. K., "Drag Measurements in Roughness Arrays of Varying Density and Distribution," *Agric. Meteor.*, Vol. 8, 1971, pp. 269-292.

Mirels, H., "Blowing Model for Turbulent Boundary-Layer Ingestion," *AIAA J.*, Vol. 22, 1984, pp. 1582-1589.

Morris, P. J., *Forest Blowdown from Nuclear Airblast*, Defense Nuclear Agency, Washington, DC, DNA 3054F, 1973.

North Dakota Agricultural Statistics Service, *North Dakota Agricultural Statistics, 1988*, Report No. 57, North Dakota Agricultural Statistics Service, Fargo, North Dakota, 1988.

Oda, K., Suzuki, M., and T. Udagawa, "Varietal Analysis of Physical Characters in Wheat and Barley Plants Relating to Lodging and Lodging Index," *Bull. Nat. Inst. Agri. Sci.*, Series D, No. 15, 1966, pp. 55-91, (in Japanese with English summary).

Omodt, H. W., et al., *The Major Soils of North Dakota*, Bulletin No. 472, Department of Soils, Agricultural Experiment Station, North Dakota State University, Fargo, January 1968.

Owen, P. R., "Saltation of Uniform Grains in Air," *J. Fluid Mech.*, Vol. 20, 1964, pp. 225-242.

Rosenblatt, M., *Introduction to Nuclear Dust/Debris Cloud Formation*, Defense Nuclear Agency, Washington, DC, DNA 5832T, 1981.

Schlamp, R. J., K. L. Schuckman, and M. Rosenblatt, *Sweep-Up Layer Characteristics After a 1 Megaton Burst at HOB = 1000 Feet*, CRT 5360-1T, California Research and Technology, Woodland Hills, California, 1982.

Schlichting, H., *Boundary Layer Theory*, McGraw-Hill Book Co., New York, New York, 1968.

Shinn, J. H., et al., "Observations of Dust Flux in the Surface Boundary Layer for Steady and Nonsteady Cases," in R. J. Englemann and G. A. Sehmel (eds.), *Atmosphere-Surface Exchange of Particulate and Gaseous Pollutants (1974)*, Technical Information Center, U.S.Department of Energy, 1976.

Versteegen, P., D. Rault, and R. Hillendahl, *Effects of ICBM Basing, Vol. 5: Thermal Layer Experiments and Model Development*, Defense Nuclear Agency, Washington, D.C., DNA-TR-87-171-V5, December 1989.

Versteegen, P., private communication, Science Applications International Corporation, McLean, Virginia, 1989.

Westphal, D. L., O. B. Toon, and T. N. Carlson, "A Two-Dimensional Numerical Investigation of the Dynamics and Microphysics of Saharan Dust Storms," *J. Geophys. Res.*, Vol. 92, 1987, pp. 3027-3049.

DISTRIBUTION LIST

DNA-TR-90-71

DEPARTMENT OF DEFENSE

ASSISTANT TO THE SECRETARY OF DEFENSE
ATTN. EXECUTIVE ASSISTANT

DEFENSE INTELLIGENCE AGENCY
ATTN. D SUNSHINE
ATTN: DT-2A G WEBER
ATTN: RTS-2B

DEFENSE NUCLEAR AGENCY
ATTN SPSD
ATTN: SPWE C GALLOWAY
ATTN. TDTR
2 CYS ATTN: TITL

DEFENSE NUCLEAR AGENCY
ATTN: TDNM
2 CYS ATTN: TDTT W SUMMA

DEFENSE TECHNICAL INFORMATION CENTER
2 CYS ATTN: DTIC/FDAB

STRATEGIC AND THEATER NUCLEAR FORCES
ATTN: DR E SEVIN

THE JOINT STAFF
ATTN: JAD/SFD
ATTN. J8 NUC FORCE ANAL DIV

DEPARTMENT OF THE ARMY

DEP CH OF STAFF FOR OPS & PLANS
ATTN DAMO-NCZ

HARRY DIAMOND LABORATORIES
ATTN. SLCHD-NW-P-CORRIGAN

U S ARMY ATMOSPHERIC SCIENCES LAB
ATTN. SLCAS-AR-M R SUTHERLAND

U S ARMY BALLISTIC RESEARCH LAB
ATTN SLCBR-SS-T
ATTN: SLCBR-TB-B G BULMASH

U S ARMY ENGR WATERWAYS EXPER STATION
ATTN: C WELCH CEWES-SE-R
ATTN D RICKMAN CEWES-SE-R
ATTN: E JACKSON CEWES-SD-R
ATTN. F DALLRIVA CEWES-SS-R
ATTN J BALSARA CEWES-SS-R

U S ARMY NUCLEAR & CHEMICAL AGENCY
ATTN MONA-NU D BASH

U S ARMY NUCLEAR EFFECTS LABORATORY
ATTN ATAA-TDC R BENSON

DEPARTMENT OF THE NAVY

NAVAL RESEARCH LABORATORY
ATTN: CODE 2627
ATTN: CODE 4770 G COOPERSTEIN
ATTN: CODE 7920 A WILLIAMS

NAVAL SURFACE WARFARE CENTER
ATTN K42 L VALGE

NAVAL WEAPONS EVALUATION FACILITY
ATTN: CLASSIFIED LIBRARY

OFFICE OF CHIEF OF NAVAL OPERATIONS
ATTN: OP 654

DEPARTMENT OF THE AIR FORCE

AERONAUTICAL SYSTEMS DIVISION
ATTN. ASD/ENSSS H GRIFFIS

AIR UNIVERSITY LIBRARY
ATTN: AUL-LSE

BALLISTICS SYSTEMS DIVISION/MY
ATTN: ASMS
ATTN: MYE

FOREIGN TECHNOLOGY DIVISION
ATTN. SDMDA S SPRING

HQ USAF/XOXFS
ATTN: AFXOOTS

PHILLIPS LABORATORY
ATTN: HO R DUFFNER
ATTN: NTA A SHARP
ATTN: NTCA
ATTN: NTED J RENICK
ATTN: NTES

WRIGHT RESEARCH & DEVELOPMENT CENTER
ATTN: WRDC/MLBT W F ANSFACH

DEPARTMENT OF ENERGY

DEPARTMENT OF ENERGY
OFFICE OF MILITARY APPLICATIONS
ATTN. OMA/DP-225

LAWRENCE LIVERMORE NATIONAL LAB
ATTN. L-262 PAUL GUDIKSEN
ATTN: L-439 J KELLER
ATTN: L-81 R PERRETT
ATTN L-85 P CHRZANOWSKI

LOS ALAMOS NATIONAL LABORATORY
ATTN A S MASON
ATTN· J NORMAN
ATTN. R W SELDEN
ATTN. R W WHITAKER
ATTN: R S DINGUS

SANDIA NATIONAL LABORATORIES
ATTN· A CHABAI DIV 9311

OTHER GOVERNMENT

CENTRAL INTELLIGENCE AGENCY
ATTN. OSWR/NED
ATTN OSWR S WALLENHORST

DEPARTMENT OF DEFENSE CONTRACTORS

ACUREX CORP
ATTN C NARDO

AEROJET PROPULSION DIVISION
ATTN· A COLLINS

AEROSPACE CORP
ATTN D RAUSCH
ATTN H BLAES M2 250
ATTN· L SELZER M4/925

APPLIED RESEARCH ASSOCIATES, INC
ATTN. J KEEFER

APTEK, INC
ATTN T MEAGHER

BOEING TECHNICAL & MANAGEMENT SVCS, INC
ATTN· R BURWELL

CALIFORNIA RESEARCH & TECHNOLOGY, INC
ATTN. K KREYENHAGEN

CALIFORNIA RESEARCH & TECHNOLOGY, INC
ATTN J THOMSEN

CALSPAN CORP
ATTN M DUNN
ATTN· M HOLDEN

CARPENTER RESEARCH CORP
ATTN H J CARPENTER

G B LABORATORY, INC
ATTN G BURGHART

GENERAL ATOMICS, INC
ATTN CHARLES CHARMAN

GENERAL ELECTRIC CO
ATTN B MAGUIRE

GENERAL RESEARCH CORP
ATTN W ADLER

H & H CONSULTANTS, INC
ATTN W HALL

HERCULES, INC
ATTN. P MCALLISTER

HORIZONS TECHNOLOGY, INC
ATTN: W T KREISS

INSTITUTE FOR DEFENSE ANALYSES
ATTN. CLASSIFIED LIBRARY
ATTN: E BAUER

JAYCOR
ATTN. W FLATHAU

KAMAN SCIENCES CORP
ATTN R RUETENIK
ATTN· T STAGLIANO

KAMAN SCIENCES CORP
ATTN: F SHELTON
ATTN B KINSLOW

KAMAN SCIENCES CORP
ATTN D MOFFETT
ATTN DASIAC

KAMAN SCIENCES CORPORATION
ATTN: DASIAC

LACHEL PIEPENBURG AND ASSOCIATES, INC
ATTN· D PIEPENBURG

LOCKHEED MISSILES & SPACE CO, INC
ATTN. P J SCHNEIDER
ATTN· R K JAMISON
ATTN. T J KELIHER

MCDONNELL DOUGLAS CORPORATION
ATTN. L COHEN

PACIFIC-SIERRA RESEARCH CORP
2 CYS ATTN: R A GAJ
2 CYS ATTN R SMALL

R & D ASSOCIATES
ATTN· R ROSS
ATTN. T A MAZZOLA

R & D ASSOCIATES
ATTN G GANONG

R & D ASSOCIATES
ATTN. J WEBSTER

RAND CORP
ATTN· LIBRARY

S-CUBED
ATTN C NEEDHAM

SCIENCE APPLICATIONS INTL CORP
ATTN J STODDARD

SCIENCE APPLICATIONS INTL CORP
ATTN. D BACON
ATTN. J COCKAYNE
ATTN· P VERSTEEGEN
ATTN. W LAYSON

SCIENCE APPLICATIONS INTL CORP
ATTN J MANSHIP

SOUTHERN RESEARCH INSTITUTE
ATTN. C PEARS

SRI INTERNATIONAL
ATTN J COLTON
ATTN· M SANAI

TECH REPS, INC
ATTN· F MCMULLAN

TOYON RESEARCH CORP
ATTN· J CUNNINGHAM

TRW INC
ATTN: A ZIMMERMAN
ATTN M SEIZEW
ATTN· P BRANDT
ATTN. R BACHARACH

WEIDLINGER ASSOC, INC
ATTN. DARREN TENNANT
ATTN: H LEVINE

WEIDLINGER ASSOCIATES, INC
ATTN· M BARON